

Spin Crossover in a Vacuum-Deposited Submonolayer of a Molecular Iron(II) Complex

Matthias Bernien,^{*,†} Dennis Wiedemann,^{*,‡} Christian F. Hermanns,[†] Alex Krüger,[†] Daniela Rolf,[†] Wolfgang Kroener,[§] Paul Müller,[§] Andreas Grohmann,[‡] and Wolfgang Kuch[†]

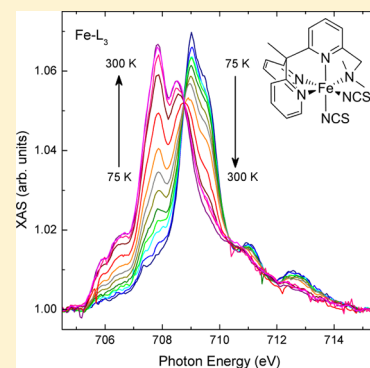
[†]Institut für Experimentalphysik, Freie Universität Berlin, Arnimallee 14, 14195 Berlin, Germany

[‡]Institut für Chemie, Technische Universität Berlin, Straße des 17. Juni 135, 10623 Berlin, Germany

[§]Department of Physics, Universität Erlangen-Nürnberg, Erwin-Rommel-Straße 1, 91058 Erlangen, Germany

Supporting Information

ABSTRACT: Spin-state switching of transition-metal complexes (spin crossover) is sensitive to a variety of tiny perturbations. It is often found to be suppressed for molecules directly adsorbed on solid surfaces. We present X-ray absorption spectroscopy measurements of a submonolayer of $[\text{Fe}^{\text{II}}(\text{NCS})_2\text{L}]$ (L: 1-{6-[1,1-di(pyridin-2-yl)ethyl]-pyridin-2-yl}-*N,N*-dimethylmethanamine) deposited on a highly oriented pyrolytic graphite substrate in ultrahigh vacuum. These molecules undergo a thermally induced, fully reversible, gradual spin crossover with a transition temperature of $T_{1/2} = 235(6)$ K and a transition width of $\Delta T_{80} = 115(8)$ K. Our results show that by using a carbon-based substrate the spin-crossover behavior can be preserved even for molecules that are in direct contact with a solid surface.



SECTION: Physical Processes in Nanomaterials and Nanostructures

Since its first observation in 1931 and rationalization using ligand-field theory in the 1950s, the spin-crossover (SCO) phenomenon has been intensely researched and discussed, particularly with regard to potential applications in information storage and processing.^{1–3} Most of the known SCO compounds are transition-metal complexes, especially $3d^4$ – $3d^7$ metal ions in pseudo-octahedral coordination, with a predominance of iron(II) in N_6 environments. Among these, (pyridine)bis(thiocyanato- κN)iron(II) complexes constitute an exceptionally well-studied class.⁴ Assemblies of such molecules have been synthesized and characterized in bulk, nanoscale, and surface phases. Typical methods for preparing the latter comprise Langmuir–Blodgett techniques, spin coating, and vacuum deposition, leading to thin or ultrathin films.^{5–8} Because the spin state of a molecule influences a multitude of its physical and chemical properties, it can be monitored using a wide variety of methods, for example, IR, Mössbauer, NMR, Raman, UV/vis, and X-ray absorption spectroscopies (XAS), conductometry, dielectrometry, diffractometry, refractometry, and susceptometry.^{9–13}

Recently, an electron-induced spin-state switching of $[\text{Fe}^{\text{II}}(\text{bpb})_2(\text{phen})]$ (bpb: bis(1*H*-pyrazol-1-yl)borate, phen: 1,10-phenanthroline) in the second molecular layer deposited on Au(111) in ultrahigh vacuum (UHV) was observed by differential tunneling spectroscopy at 5 K, but the molecules of the first layer could not be switched.¹⁴ The remarkably high sensitivity to the environment, which is typical of SCO compounds, often suppresses the switching behavior of

molecules in direct contact with a substrate. Similarly, $[\text{Fe}^{\text{II}}(\text{NCS})_2(\text{phen})_2]$ on Cu(100) does not show an SCO transition in the first molecular layer, whereas isolated $[\text{Fe}^{\text{II}}(\text{NCS})_2(\text{phen})_2]$ molecules on an interfacial layer of CuN on Cu(100) may be switched between their high-spin (HS) and low-spin (LS) state by the tunneling current at 4.6 K.¹⁵ Oligonuclear “beads” in chains of $[\text{Fe}^{\text{II}}\text{L}'_2](\text{BF}_4)_2$ (L': 2,6-di(1*H*-pyrazol-1-yl)-4-(thiocyanatomethyl)pyridine), after self-assembly on highly oriented pyrolytic graphite (HOPG) from acetonitrile solution, do show spin-state interconversion, as detected by current-imaging tunneling spectroscopy (CITS).¹⁶

Here we report on the thermally induced, reversible spin-state switching of submonolayers of the molecular complex $[\text{Fe}^{\text{II}}(\text{NCS})_2\text{L}]$ (1, Figure 1; L: 1-{6-[1,1-di(pyridin-2-yl)ethyl]-pyridin-2-yl}-*N,N*-dimethylmethanamine), obtained by vacuum deposition onto an HOPG surface. Complex 1 has a novel N_4 chelate ligand designed to contain both imine and aliphatic amine N donors and two thiocyanato- κN ligands. HOPG was chosen as substrate because it promises only weak interaction, possibly leaving the molecular properties and thus the SCO behavior largely unaffected.

Submonolayer coverages of 1 were obtained by thermal deposition at ~ 510 K from a tantalum Knudsen cell onto an HOPG substrate under UHV conditions and measured by X-

Received: August 13, 2012

Accepted: November 7, 2012

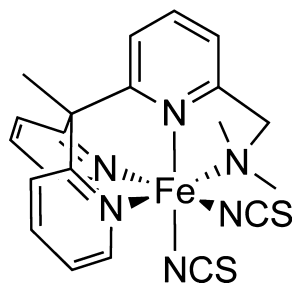


Figure 1. Structural formula of $[\text{Fe}^{\text{II}}(\text{NCS})_2\text{L}]$ (**1**).

ray absorption spectroscopy (XAS). To characterize the adsorption of **1** on the HOPG surface, we have performed low-energy electron diffraction (LEED) experiments. Figure 2 shows LEED images of the clean HOPG surface (a), 1.2 monolayer (ML) of **1** on HOPG directly (b) and after 10 min of measuring with the electron beam at the same position (c). The ring-shaped diffracted electron intensity in panel a demonstrates that the graphite surface is highly oriented, while containing crystallites of different azimuthal orientation. The disappearance of the diffraction pattern in panel b proves that the molecules wet the surface and form a molecular layer because the electrons diffracted by the HOPG substrate are strongly damped by the adsorbate. If **1** would form crystallites, then most parts of the surface would remain uncovered, and the ring-shaped diffraction pattern would be only slightly damped. Even though we cannot rule out that a minor part of the molecules may already occupy second monolayer positions while the first monolayer is not yet complete, we can conclude that **1** grows layerwise on HOPG and that no crystallites are formed. The partial reappearance of the substrate diffraction pattern in panel c is interpreted as the result of electron beam damage and subsequent partial desorption of fragments of the molecules.

Fe- $L_{2,3}$ XA spectra give direct access to detailed information on the electronic structure of the iron(II) ions, allowing for straightforward identification of the HS and LS state and their interconversion with temperature. Figure 3 shows the isotropic Fe- $L_{2,3}$ X-ray absorption spectra of 0.8 ML of **1** on HOPG measured at 300 (black) and 75 K (red). Strong temperature-dependent changes of the Fe XAS signal are evident. At room temperature, the Fe- L_3 edge displays a double-peak feature at photon energies of 707.8 and 708.5 eV. At 75 K, the Fe- L_3 edge is shifted by ~ 1.1 eV to higher photon energy and slightly compressed. These changes are accompanied by a change of the relative intensity of the Fe- L_3 (705 to 715 eV) and L_2 (718

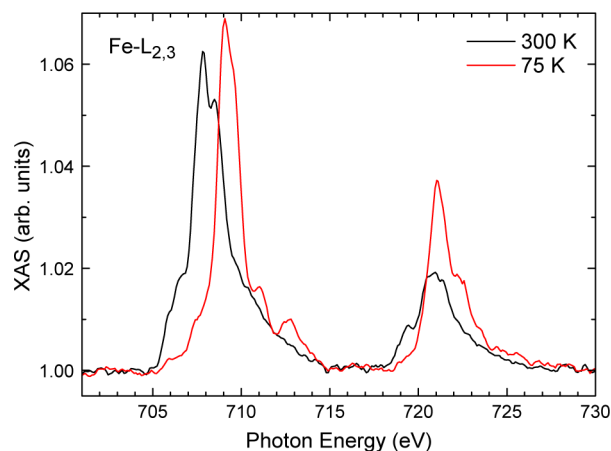


Figure 3. Temperature-dependent isotropic Fe- $L_{2,3}$ X-ray absorption spectra of 0.8 monolayers of **1** on HOPG.

to 726 eV) edge. The branching ratio, defined as the ratio of the integrated L_3 intensity and the intensities of the L_3 and the L_2 edges taken together, is reduced from 0.74(2) at 300 K to 0.64(2) at 75 K. Such a reduction is typical of an HS-to-LS transition and reflects the decrease in 3d spin-orbit coupling energy due to the vanishing magnetic moment in the LS state.^{17,18} The shapes of the Fe- $L_{2,3}$ XA spectra of both the HS and the LS state closely resemble those of $[\text{Fe}^{\text{II}}(\text{NCS})_2(\text{phen})_2]$,¹⁹ indicating that the ligand field of the Fe center is very similar for the two systems. The spin transition of 0.8 ML of **1** on HOPG appears to be nearly complete at low temperatures, and the spectra at 300 and 75 K represent almost pure HS and LS states, respectively.

The isotropic Fe- L_3 XA spectra shown in Figure S1 of the Supporting Information were recorded during heating the sample from 75 to 300 K. The spectra display a gradual transition between the two spectra presented in Figure 3. Figure 4 shows the fraction of HS molecules plotted over the temperature. For the determination of the HS fraction, each Fe- L_3 XA spectrum was fitted as a linear combination of the spectrum at 300 and at 75 K. Because the temperature-dependent spectral change is saturating at low temperatures, it can be assumed that the spectrum at 75 K represents a pure LS spin state. At 300 K, the transition to the HS state is not complete. However, the maximal LS contribution can be estimated by subtracting fractions of the spectrum at 75 K shown in Figure 2 from the one at 300 K and must be smaller than 20% because the resulting intensities cannot be smaller

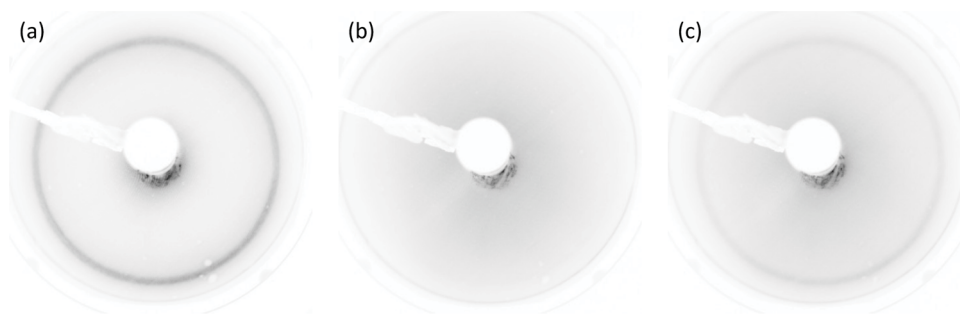


Figure 2. LEED images (contrast inverted) at 70 eV electron energy and room temperature of (a) the clean HOPG surface, (b) 1.2 ML of **1** on HOPG, acquired immediately after exposing the sample to the electron beam, and (c) the same spot of the sample after 10 min of exposure to the electron beam. The images have been taken under identical measuring conditions.

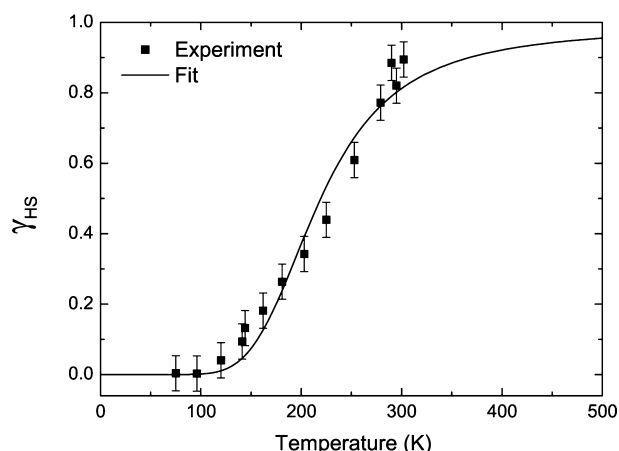


Figure 4. Fraction of HS molecules (squares) as a function of temperature and fit of a model based on noninteracting molecules.

than one. For Figure 4, an HS fraction of 90% is assumed at 300 K. The temperature at which half of the molecules are in the HS state is approximately $T_{1/2} = 235(6)$ K. The transition width defined as the temperature difference at which 80% of the molecules are in the HS and LS state, respectively, is found to be $\Delta T_{80} = 115(8)$ K.

The temperature dependence can be modeled as an SCO transition of noninteracting molecules. Because in a vacuum the energy associated with a change in volume is zero, the thermal equilibrium condition is obtained by minimizing the free energy of the ensemble of molecules.²⁰ The fraction of HS molecules is then given by

$$\gamma_{HS}(T) = \frac{1}{\exp\left(-\frac{\Delta_{SCO}S_m}{R}\right) \cdot \exp\left(\frac{\Delta_{SCO}H_m}{RT}\right) + 1}$$

where $\Delta_{SCO}H_m$ is the difference in molar enthalpy and $\Delta_{SCO}S_m$ is the difference in molar entropy between the HS and LS states. The fit of this model to the experimental data is shown in Figure 4 (solid line) and yields $\Delta_{SCO}H_m = 10.0(10)$ kJ·mol⁻¹ and $\Delta_{SCO}S_m = 45(5)$ J·K⁻¹·mol⁻¹. Because the transition is virtually complete below 90 K, we conclude that also those molecules in direct contact with the HOPG surface undergo the spin transition. Superconducting quantum-interference device (SQUID) susceptometry of a powder sample has been conducted to compare surface and bulk behavior. We found that a typical, gradual, complete, one-step SCO without hysteresis—very similar to the one in structurally related [Fe(dpea)(NCS)₂] (dpea: [2-aminoethyl]bis[2-pyridylmethyl]amine)²¹—takes place at $T_{1/2} = 251(3)$ K, exhibiting a transition width of $\Delta T_{80} = 62(4)$ K. Fitting the model mentioned above to the bulk data yields thermodynamic parameters of $\Delta_{SCO}H_m = 22.8(5)$ kJ·mol⁻¹ and $\Delta_{SCO}S_m = 92(2)$ J·K⁻¹·mol⁻¹ (Figure S2 of the Supporting Information). These values indicate less cooperativity between the molecules on the surface than in the powder (resulting in a broader transition), an enthalpically less preferred LS state, and an entropically less preferred HS state on the surface compared with the bulk material. The latter fact as well as a somewhat better fit of the bulk behavior to the simple noninteraction model ($R^2 = 0.9983$ compared with 0.9710 for the surface phase) suggests an interaction between molecules and surface that does, however, not quench the SCO. Along with the absence of cooperativity, this further hints at a wetting of the surface rather than cluster

formation. As expected for an SCO transition, the spin of the Fe centers of **1** on HOPG can be switched repeatedly and in a fully reversible manner between HS and LS by altering the temperature (Figure S3 of the Supporting Information).

In conclusion, a thermally induced, reversible SCO transition has been demonstrated for a submonolayer of [Fe^{II}(NCS)₂L] molecules thermally deposited in UHV on an HOPG surface. The HS and LS spin states could be clearly identified by means of XAS at the Fe-L_{2,3} edges. The SCO transition is nearly complete and shows a very gradual behavior between 90 and 300 K, indicating that the transition acts on the single-molecule level with a low degree of cooperativity. Our result may serve as proof of principle that the quenching of switching of surface-mounted molecular units can be overcome by using carbon-based surfaces. This opens up new possibilities to realize the vision of highly sensitive SCO molecules serving as tools for creating molecular spintronic devices on surfaces. It remains interesting to see if unquenched switching behavior can also be found on graphene surfaces.

EXPERIMENTAL SECTION

Ligand L was synthesized by Eschweiler–Clarke methylation of the corresponding primary amine, {6-[1,1-di(pyridin-2-yl)-ethyl]pyridin-2-yl}methanamine,²² following a standard literature procedure.²³ It was purified by column chromatography and subsequently reacted with [Fe(NCS)₂(py)₄]²⁴ (py: pyridine) in methanol to give pure [Fe(NCS)₂L] (**1**) in a yield of 73% (see Supporting Information). Solid-state variable-temperature magnetic susceptibility measurements were performed using a Quantum Design MPMS-XLS SQUID magnetometer operating at 0.1 T. Diamagnetic corrections for the sample and the sample holder were applied.

LEED images were taken using an Omicron Spectrae system with a spot size of the electron beam of ~ 0.5 mm in diameter and a sample current of ~ 0.8 μ A during the measurement. We purchased $10 \times 10 \times 2$ mm³ SPI-1 high-grade HOPG substrates exhibiting a mosaic angle of $0.4 \pm 0.1^\circ$ from Structure Probe. A clean HOPG surface was obtained by cleaving an HOPG substrate at a pressure of 10^{-6} mbar by means of a carbon tape. The quality of the HOPG surface was checked by the angle dependence of the C π^* resonance at 285.4 eV. Successful preparations typically showed a ratio of 1:100 between the resonance intensity for vertically s- and horizontally p-polarized X-rays at 20° grazing incidence. Cleavage was repeated if the ratio was larger. **1** was deposited at ~ 510 K from a tantalum Knudsen cell at 5×10^{-9} mbar onto the substrate held at room temperature. Coverages were determined by using a quartz microbalance and the absolute Fe-L_{2,3} XAS intensity. After deposition, the sample was heated to 350 K to desorb volatile nitrogen-containing fragments produced during the deposition process. These fragments are likely L, which decoordinates at 460 K in high vacuum (Figure S4 of the Supporting Information). After desorption, only intact molecules of compound **1** remain on the surface, as concluded from the observation that the spin transition is complete at low temperatures. XAS measurements were performed at the beamline UE56/2-PGM1 at BESSY II at a pressure of 5×10^{-10} mbar. Fe-L_{2,3} isotropic XA spectra were recorded at the magic angle (54.7°) between the X-ray wave vector and the surface using linearly p-polarized X-rays. At this angle, the XAS resonance intensities are independent of the orientations of the molecular orbitals.²⁵ The energy resolution was set to 300 meV at a photon flux of $\sim 10^{13}$ photons s⁻¹ cm⁻².

XA spectra were acquired in total-electron-yield mode by recording the sample drain current as a function of photon energy. The XAS signal of the sample was normalized to the one of a gold grid upstream to the experiment that was recorded in parallel. Subsequently, the spectra were normalized to the substrate signal approximated by a linear function. Time-dependent X-ray-induced irreversible modifications of the Fe-L₃ edge structure lead to apparent reduction of the HS contribution of 20% within 1 h of continuous illumination at room temperature with three times the flux density used for recording the spectra (Figure S5 of the Supporting Information). Consequently, the measuring time for each spectrum was limited to 3 min before a new position on the sample was chosen. On this time scale, the spectra at room temperature and at low temperatures showed no time-dependent variations so that chemical modifications of the molecules as well as an X-ray-induced formation of crystallites can be ruled out.

■ ASSOCIATED CONTENT

● Supporting Information

Synthesis of **1**, XAS and SQUID measurements of powder samples of **1**, mass spectra of pristine and sublimated **1**, and X-ray dosage-dependent XAS measurements of a submonolayer of **1** on HOPG. This material is available free of charge via the Internet at <http://pubs.acs.org/>.

■ AUTHOR INFORMATION

Corresponding Authors

*E-mail: bernien@physik.fu-berlin.de.

*E-mail: dennis.wiedemann@chem.tu-berlin.de.

Notes

The authors declare no competing financial interest.

■ ACKNOWLEDGMENTS

W. Mahler and W. Walter are acknowledged for their support during the XAS measurements. Financial support by the DFG (Sfb 658: Elementary Processes in Molecular Switches on Surfaces) is gratefully acknowledged.

■ REFERENCES

- (1) Cambi, L.; Szegő, L. Über die magnetische Suszeptibilität der komplexen Verbindungen. *Ber. Dtsch. Chem. Ges.* **1931**, *64*, 2591–2598.
- (2) Griffith, J. S.; Orgel, L. E. Ligand-Field Theory. *Q. Rev. Chem. Soc.* **1957**, *11*, 381–393.
- (3) Létard, J.-F.; Guionneau, P.; Goux-Capes, L. In *Spin Crossover in Transition Metal Compounds III*; Gülich, P., Goodwin, H. A., Eds.; Springer: Berlin, 2004; pp 221–249.
- (4) Guionneau, P.; Marchivie, M.; Bravic, G.; Létard, J.-F.; Chasseau, D. In *Spin Crossover in Transition Metal Compounds II*; Gülich, P., Goodwin, H. A., Eds.; Springer: Berlin, 2004; pp 97–128.
- (5) Soyer, H.; Dupart, E.; Gómez-García, C. J.; Mingotaud, C.; Delhaès, P. First Magnetic Observation of a Spin Crossover in a Langmuir-Blodgett Film. *Adv. Mater.* **1999**, *11*, 382–384.
- (6) Matsuda, M.; Tajima, H. Thin Film of a Spin Crossover Complex [Fe(dpp)₂](BF₄)₂. *Chem. Lett.* **2007**, *36*, 700–701.
- (7) Naggert, H.; Bannwarth, A.; Chemnitz, S.; von Hofe, T.; Quandt, E.; Tuczek, F. First Observation of Light-Induced Spin Change in Vacuum Deposited Thin Films of Iron Spin Crossover Complexes. *Dalton Trans.* **2011**, *40*, 6364–6366.
- (8) Palamarciuc, T.; Oberg, J. C.; El Hallak, F.; Hirjibehedin, C. F.; Serri, M.; Heutz, S.; Létard, J.-F.; Rosa, P. Spin Crossover Materials Evaporated under Clean High Vacuum and Ultra-High Vacuum

Conditions: from Thin Films to Single Molecules. *J. Mater. Chem.* **2012**, *22*, 9690–9695.

- (9) Gülich, P.; Hauser, A.; Spiering, H. Thermal and Optical Switching of Iron(II) Complexes. *Angew. Chem., Int. Ed.* **1994**, *33*, 2024–2054.
- (10) Félix, G.; Abdul-Kader, K.; Mahfoud, T.; Gural'skiy, I. A.; Nicolazzi, W.; Salmon, L.; Molnár, G.; Bousseksou, A. Surface Plasmons Reveal Spin Crossover in Nanometric Layers. *J. Am. Chem. Soc.* **2011**, *133*, 15342–15345.
- (11) Rotaru, A.; Gural'skiy, I. A.; Molnár, G.; Salmon, L.; Demont, P.; Bousseksou, A. Spin State Dependence of Electrical Conductivity of Spin Crossover Materials. *Chem. Commun.* **2012**, *48*, 4163–4165.
- (12) Bonhommeau, S.; Guillon, T.; Lawson Daku, L. M.; Demont, P.; Sanchez Costa, J.; Létard, J.-F.; Molnár, G.; Bousseksou, A. Photoswitching of the Dielectric Constant of the Spin-Crossover Complex [Fe(L)(CN)₂]₂·H₂O. *Angew. Chem., Int. Ed.* **2006**, *45*, 1625–1629.
- (13) Real, J. A.; Castro, I.; Bousseksou, A.; Verdaguer, M.; Burriel, R.; Castro, M.; Linares, J.; Varret, F. Spin Crossover in the 2,2'-Bipyrimidine- (bpym-) Bridged Iron(II) Complexes [Fe(L)-(NCX)₂]₂(bpym) (L = 2, 2'-Bithiazoline (bt) and bpym; X = S, Se). X-ray Absorption Spectroscopy, Magnetic Susceptibility, Calorimetric, and Mössbauer Spectroscopy Studies. *Inorg. Chem.* **1997**, *36*, 455–464.
- (14) Gopakumar, T. G.; Matino, F.; Naggert, H.; Bannwarth, A.; Tuczek, F.; Berndt, R. Electron-Induced Spin Crossover of Single Molecules in a Bilayer on Gold. *Angew. Chem., Int. Ed.* **2012**, *51*, 6262–6266.
- (15) Miyamachi, T.; Gruber, M.; Davesne, V.; Bowen, M.; Boukari, S.; Joly, L.; Scheurer, F.; Rogez, G.; Yamada, T. K.; Ohresser, P.; et al. Robust Spin Crossover and Memristance across a Single Molecule. *Nat. Commun.* **2012**, *3*, 938.
- (16) Alam, M. S.; Stocker, M.; Gieb, K.; Müller, P.; Haryono, M.; Student, K.; Grohmann, A. Spin-State Patterns in Surface-Grafted Beads of Iron(II) Complexes. *Angew. Chem., Int. Ed.* **2010**, *49*, 1159–1163.
- (17) Thole, B. T.; van der Laan, G. Branching Ratio in X-Ray Absorption Spectroscopy. *Phys. Rev. B* **1988**, *38*, 3158–3171.
- (18) van der Laan, G.; Kirkman, I. W. The 2p Absorption Spectra of 3d Transition Metal Compounds in Tetrahedral and Octahedral Symmetry. *J. Phys.: Condens. Matter* **1992**, *4*, 4189–4204.
- (19) CartierditMoulin, C.; Rudolf, P.; Flank, A. M.; Chen, C. T. Spin Transition Evidenced by Soft X-ray Absorption Spectroscopy. *J. Phys. Chem.* **1992**, *96*, 6196–6198.
- (20) Adler, P.; Wiehl, L.; Meibner, E.; Köhler, C.; Spiering, H.; Gülich, P. The Influence of the Lattice on the Spin Transition in Solids. Investigations of the High Spin ⇌ Low Spin Transition in Mixed Crystals of [Fe_xM_{1-x}(2-pic)₃]Cl₂·MeOH. *J. Phys. Chem. Solids* **1987**, *48*, 517–525.
- (21) Matouzenko, G. S.; Bousseksou, A.; Lecocq, S.; van Koningsbruggen, P. J.; Perrin, M.; Kahn, O.; Collet, A. Spin Transition in [Fe(DPEA)(NCS)₂], a Compound with the New Tetradentate Ligand (2-Aminoethyl)bis(2-pyridylmethyl)amine (DPEA): Crystal Structure, Magnetic Properties, and Mössbauer Spectroscopy. *Inorg. Chem.* **1997**, *36*, 2975–2981.
- (22) Ünal, E. A.; Wiedemann, D.; Seiffert, J.; Boyd, J. P.; Grohmann, A. Efficient Synthesis of Pentakis- and Tris(pyridine) Ligands. *Tetrahedron Lett.* **2012**, *53*, 54–55.
- (23) Clarke, H. T.; Gillespie, H. B.; Weisshaus, S. Z. The Action of Formaldehyde on Amines and Amino Acids. *J. Am. Chem. Soc.* **1933**, *55*, 4571–4587.
- (24) Erickson, N. E.; Sutin, N. The So-Called cis-trans Isomerism of Bis(isothiocyanato) Tetra(pyridine) Iron(II). *Inorg. Chem.* **1966**, *5*, 1834–1835.
- (25) Stöhr, J.; Outka, D. A. Determination of Molecular Orientations on Surfaces from the Angular Dependence of Near-Edge X-Ray-Absorption Fine-Structure Spectra. *Phys. Rev. B* **1987**, *36*, 7891–7905.